

Atherosclerotic Lesions Rich in Macrophages or Smooth Muscle Cells Discriminated in Rabbit Iliac Arteries Based on T1 Relaxation Time and Lipid Content

Yasuyoshi Kuroiwa, MS, Atsushi Yamashita, MD, PhD, Tosiaki Miyati, PhD, DMSc, Eiji Furukoji, MD, PhD, Misaki Takahashi, MS, Toshiya Azuma, PhD, Hiroshi Sugimura, MD, PhD, Shozo Tamura, MD, PhD, Keiichi Kawai, PhD, Yujiro Asada, MD, PhD

Rationale and Objectives: Atherothrombosis usually occurs on macrophage- and lipid-rich unstable plaque, but rarely on smooth muscle cell (SMC)-rich stable plaque. Magnetic resonance imaging (MRI) has been extensively applied for noninvasive vascular imaging. We therefore investigated whether MRI provides valuable information about the characteristics of atherosclerotic vessels using rabbit models of macrophage-rich or SMC-rich atherosclerotic arteries.

Materials and Methods: Rabbits were fed with a conventional (CD group, $n = 3$) or 0.5% cholesterol (ChD group, $n = 3$) diet for 1 week before and 3 weeks after balloon injury of the left iliac arteries. Three weeks later, these arteries were investigated by 1.5 T MRI and by conventional angiographic imaging, followed by histological and immunohistochemical analyses.

Results: Three weeks after balloon injury, injured iliac arteries of both groups formed neointima with luminal stenosis. Conventional and MRI angiographic findings of the luminal diameter significantly and positively correlated. T1 relaxation time was significantly shorter and the lipid content was much higher in injured arteries from the ChD than from the CD group. The injured arteries from the ChD also contained more macrophages and less SMCs than those from the CD group. The T1 relaxation time and lipid content in injured arteries negatively and positively correlated with the degree of macrophage accumulation, respectively.

Conclusion: These results showed that MRI could provide valuable information about luminal stenosis and the characteristics of atherosclerotic vessels in rabbits.

Key Words: Magnetic resonance imaging; atherosclerosis; macrophage; smooth muscle cell.

©AUR, 2010

Thrombus formation after atherosclerotic plaque disruption is a major cause of acute coronary syndrome and stroke. Atherothrombosis usually occurs on macrophage- and lipid-rich unstable plaque, but rarely on smooth muscle cell (SMC)-rich stable plaque (1). Beside luminal stenosis, plaque composition and morphology are

key determinants of whether a plaque will cause cardiovascular events. Despite major advances in treatment, a high ratio of apparently healthy and asymptomatic patients dies of atherosclerosis (2). Therefore the development of screening and diagnostic methods to identify and characterize plaque composition is very important to determine the patient-specific risk of cardiovascular events and improve treatment strategies.

Magnetic resonance imaging (MRI) is used extensively for noninvasive vascular imaging, because it can identify components of atherosclerotic plaques such as a lipid-rich/necrotic core, calcification, and hemorrhage (3,4). It can also visualize and quantify lipid-rich human carotid plaque (5–7) and the rabbit aorta (8). However, whether or not MRI can distinguish between stable and unstable atherosclerotic vessels in vivo is unknown. The aim of the study is to investigate whether MRI can distinguish between rabbit iliac arteries with macrophage-rich and SMC-rich atherosclerotic lesions.

Acad Radiol 2010; 17:230–238

From the Department of Radiological Technology, Koga General Hospital, Miyazaki (Y.K.); Departments of Pathology (Y.K., A.Y., M.T., Y.A.) and of Radiology (E.F., T.A., H.S., S.T.), Faculty of Medicine, University of Miyazaki, 5200 Kihara, Kiyotake, Miyazaki 889-1692, Japan; Division of Health Sciences, Graduate School of Medical Science, Kanazawa University, Ishikaw (Y.K., T.M., T.A., K.K.); and Biomedical Imaging Research Center, University of Fukui, Fukui, Japan (K.K.). Received June 24, 2009; accepted September 8, 2009. **Address correspondence to:** Y.A. e-mail: yasada@fc.miyazaki-u.ac.jp

©AUR, 2010

doi:10.1016/j.acra.2009.09.008

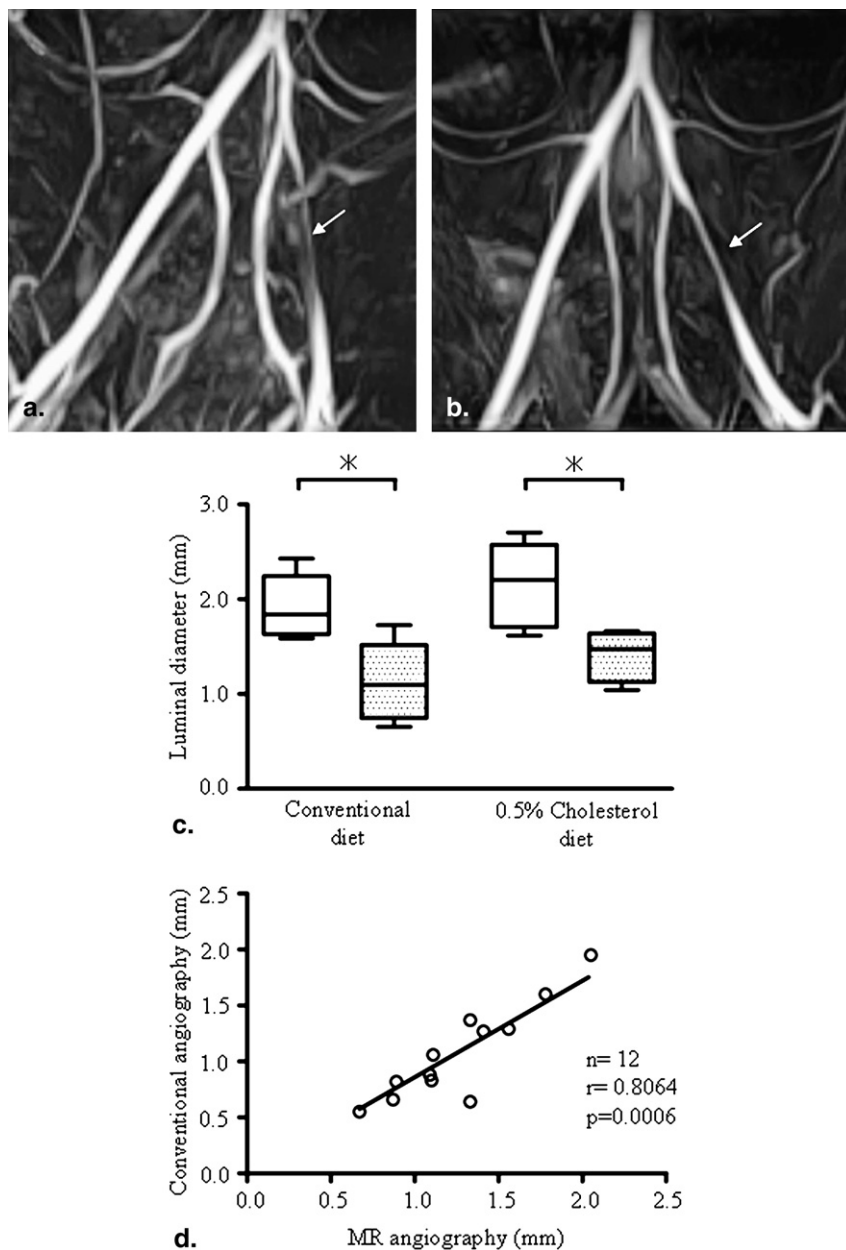


Figure 1. Representative magnetic resonance (MR) angiograms of rabbit iliac arteries. MR angiograms of the conventional cholesterol group (CD) (**a**) and 0.5% cholesterol group (ChD) (**b**) rabbits. Injured iliac arteries (*left*) of both groups have a narrower lumen (*arrows*) than uninjured arteries. (**c**) Luminal diameters of uninjured arteries (*open box*) and 3 weeks (*dotted box*) after balloon injury. ($n = 6$ each; $*P < .001$). Data are presented as medians (*horizontal bar*), quartile ranges (*boxes*), and 90th percentiles (*error bars*). (**d**) Linear regression analysis of associations between conventional and MR angiography with respect to luminal diameter.

MATERIALS AND METHODS

Experimental Design

Six male Japanese white rabbits weighing 2.5–3.0 kg were fed with a conventional diet (CD group; $n = 3$) or a 0.5% cholesterol diet (ChD group; $n = 3$) for 1 week before and 3 weeks after balloon injury. All surgical manipulations proceeded under aseptic conditions and general anesthesia elicited by an intravenous injection of pentobarbital (25 mg/kg, body weight). One week after starting the diets, an angioplasty balloon catheter (2.75-mm diameter, 18-mm length; Potenza, Japan Lifeline Co, Osaka, Japan) was inserted via the carotid artery into the left iliac arteries under fluoroscopic guidance. The catheter was inflated to 1.5 atm (balloon-to-artery ratio; 1.1:1 to 1.2:1) and retracted by 5 cm three times to denude the

endothelium (9). Three weeks after balloon injury, the iliac arteries were visualized by MRI and conventional angiography, and the images were analyzed at 4-mm intervals. Immediately after conventional angiography, the rabbits were injected with heparin (500 U/kg, IV) and then killed with an overdose of pentobarbital (60 mg/kg, IV) 5 minutes later. The animals were perfused with 50 mL of 0.01 mol/L phosphate buffered saline and then perfusion-fixed with 4% paraformaldehyde for histological and immunohistochemical evaluation.

The Animal Care Committees of our institutions approved our animal research protocols. This investigation also conformed to the Guide for the Care and Use of Laboratory Animals published by the US National Institutes of Health.

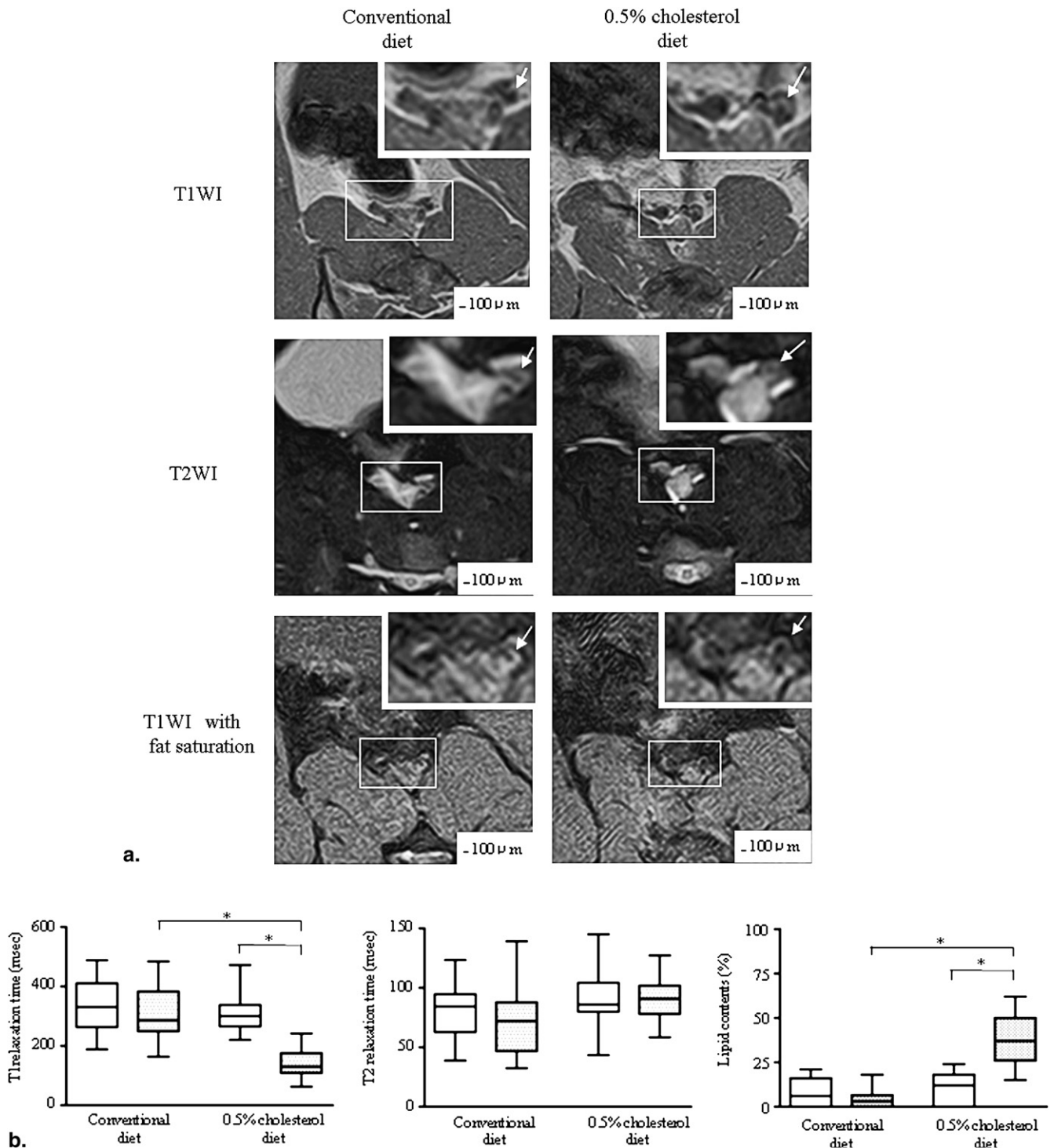


Figure 2. In vivo axial magnetic resonance (MR) images and MR parameters of rabbit iliac arteries. **(a)** Luminal narrowing appears as thicker walls in injured arteries (*arrows*) of both groups compared with uninjured arteries. Thickened artery of 0.5% cholesterol (ChD) rabbit shows low- or high-signal intensity in T1-weighted image with or without fat saturation, respectively. **(b)** T1 and T2 relaxation times and lipid contents of iliac arteries in the conventional cholesterol (CD) and ChD groups, uninjured arteries (open box) and 3 weeks after balloon injury (*dotted box*) ($n = 6$ each; $*P < .001$). Data are shown as medians (*horizontal bar*), quartile ranges (*boxes*), and 90th percentiles (*error bars*).

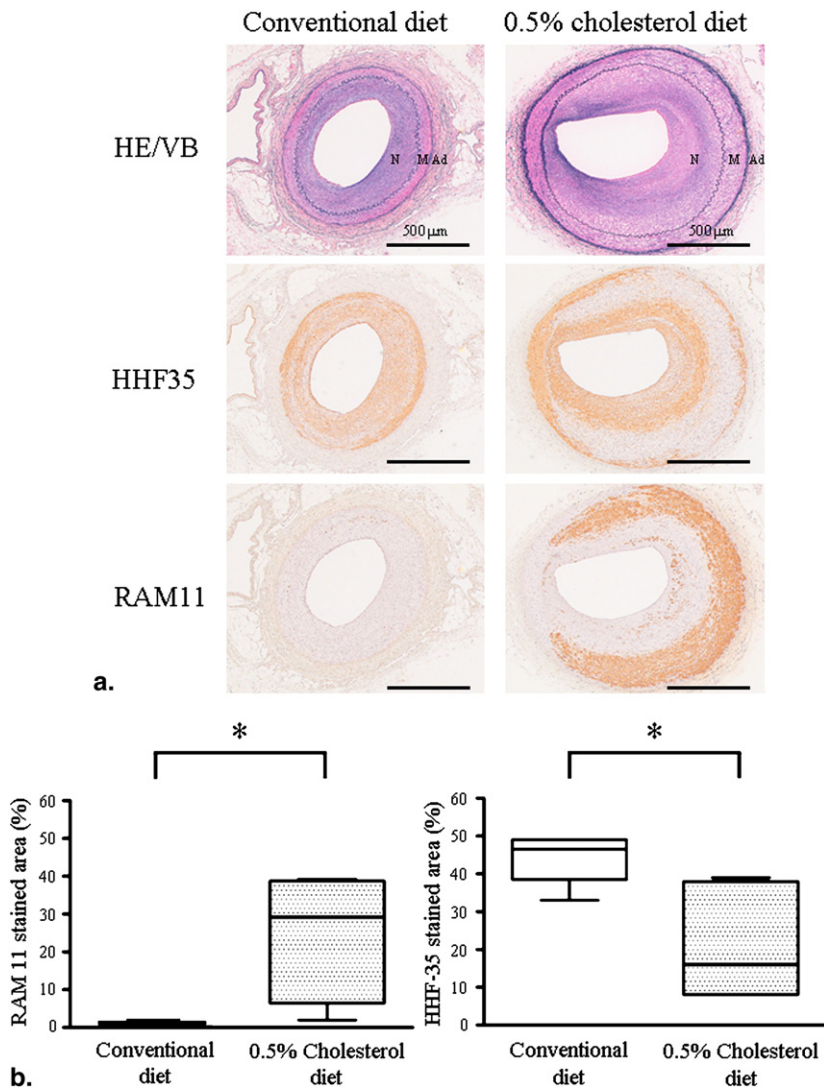


Figure 3. Representative microphotographs and linear regression analyses of iliac arteries 3 weeks after balloon injury. **(a)** Microphotographs of injured iliac arteries in both groups. Neointima has formed in injured iliac arteries. N: neointima; M: media; Ad: adventitia. **(b)** Immunopositive areas for RAM11 and HHF35 of iliac arteries 3 weeks after balloon injury in both groups ($n = 6$ each; $*P < .05$). Data are presented as medians (horizontal bar), quartile ranges (boxes), and 90th percentiles (error bars). **(c)** Linear regression analysis of associations between relaxation times and immunopositive areas in injured iliac arteries.

MRI

Three weeks after the first injury, rabbits were anesthetized and placed in the supine position in a 1.5-T superconductive magnet unit (Excelart Vantage XGV Power Plus Package, Toshiba Medical Systems, Tokyo, Japan) using a quadrature knee radiofrequency coil, then MRI proceeded with the rabbits in the left decubitus position. The abdominal aorta and femoral artery were localized using gradient-echo coronal images. Thereafter, transverse sequential images of the iliac artery from the abdominal aorta to the femoral artery were acquired using three-dimensional (3D) time-of-flight and the following parameters: repetition time/echo time (TR/TE), 40/6.8 ms; flip angle (FA), 20° and one excitation. The MRI angiography images were reconstructed in 3D using maximum intensity projection as a post-processing tool. The luminal diameter was measured on maximum intensity projection images for comparison with conventional angiography. 3D-gradient echo T1-weighted images (T1WI) were obtained using the following parameters: TR/TE, 38/5.0 ms; FA 20° and 40°, and two excitations without

fat suppression pulses. Images of the ratio (%) of fat content were generated using fat suppression 3D-gradient echo T1WI at TR/TE, 38/5.0 ms and FA 20°. We acquired 3D fast advanced spin echo proton density-weighted and T2-weighted images at TR/TE, 2000/34 and 2000/80 ms, respectively. The pixels on the images were 0.46×0.46 mm in area, slice thickness was 1 mm, and the number of excitations was two.

Ex vivo Study

Four male Japanese white rabbits were fed with a conventional diet ($n = 2$) or a 0.5% cholesterol diet ($n = 2$) for 1 week before and 3 weeks after balloon injury of the bilateral iliac arteries. The rabbits were injected with heparin (500 U/kg, IV) 3 weeks after the balloon injury, and killed with an overdose of pentobarbital (60 mg/kg, IV) 5 minutes later. The animals were perfused with 50 mL of 0.01 mol/L phosphate buffered saline, and then the excised iliac arteries were examined by MRI at 37°C using the same parameters as the study in vivo.

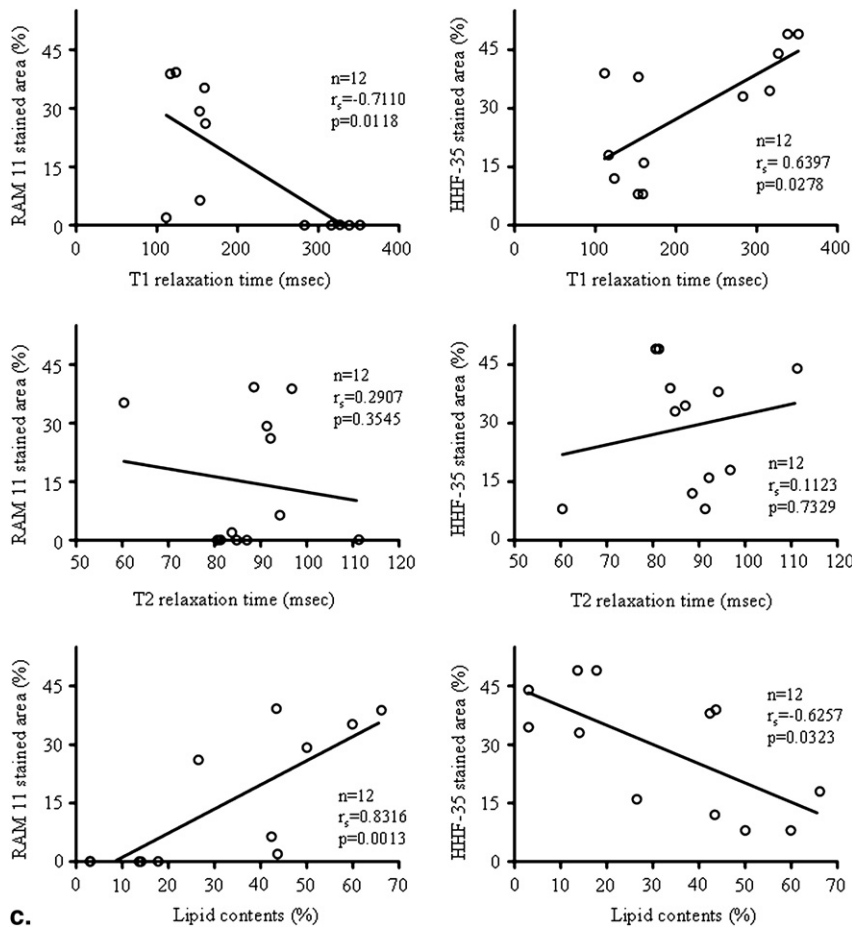


Figure 3. (continued).

Image and Data Analysis

The MRIs were transferred to a Macintosh computer for further analysis. Signal intensity (*I*) was measured on operator-defined regions of interest. The every 4-mm MRIs of iliac arteries were matched with corresponding histopathological sections of the iliac specimens. All regions of interest for each sequence were obtained on the same image to avoid variations in signal intensity. Cross-sectional areas of the lumen and the outer boundary of each iliac section were determined for both the MRIs and for the histopathological study by manual tracing with Image-J (10). Cursors for regions of interest defined by one observer were placed within iliac arteries wall to measure the T1 and T2 relaxation times. T1 and T2 were derived from the following respective equations (11):

$$T_1 = \frac{TR}{\ln\left(\frac{\sin\alpha \cdot \cos\beta \cdot I_\beta - \sin\beta \cdot \cos\alpha \cdot I_\alpha}{\sin\alpha \cdot I_\beta - \sin\beta \cdot I_\alpha}\right)}$$

$$T_2 = \frac{TE_2 - TE_1}{\ln\left(\frac{I_2}{I_1}\right)}$$

Lipid content by percentage (%) was derived from the following respective equations (12):

Lipid content (%)

$$= \frac{I_{(T1W)withoutfatsaturation} - I_{(T1W)withfatsaturation}}{I_{(T1W)withoutfatsaturation}} \times 100$$

Serum Lipid Marker Sampling and Analysis

Blood samples were collected from the peripheral ear arteries of the rabbits after a 12-hour fast, before starting the cholesterol diet, and at three weeks after injury. Serum total cholesterol (TC) and triglyceride (TG) levels were measured using the Eiken T-CHO (Eiken Kagaku, Tokyo, Japan) and Triglyceride G test (Wako Chemical, Osaka, Japan) kits, respectively.

Light Microscopy and Immunohistochemistry

The iliac arteries were fixed in 4% paraformaldehyde for 24 hours at 4°C, cut into 4-mm intervals, and embedded in paraffin. Sections (3 μm thick) were morphologically evaluated by staining with hematoxylin and eosin/Victoria blue dye. Serial sections were examined immunohistochemically using the mouse monoclonal primary anti-smooth muscle actin (HHF35, Dako, Glostrup, Denmark) and anti-macrophage (RAM11, Dako) antibodies. Horse-radish peroxidase activity was visualized using 3, 3'-diaminobenzidine tetrahydrochloride, and the sections were faintly counterstained with Meyer's hematoxylin.

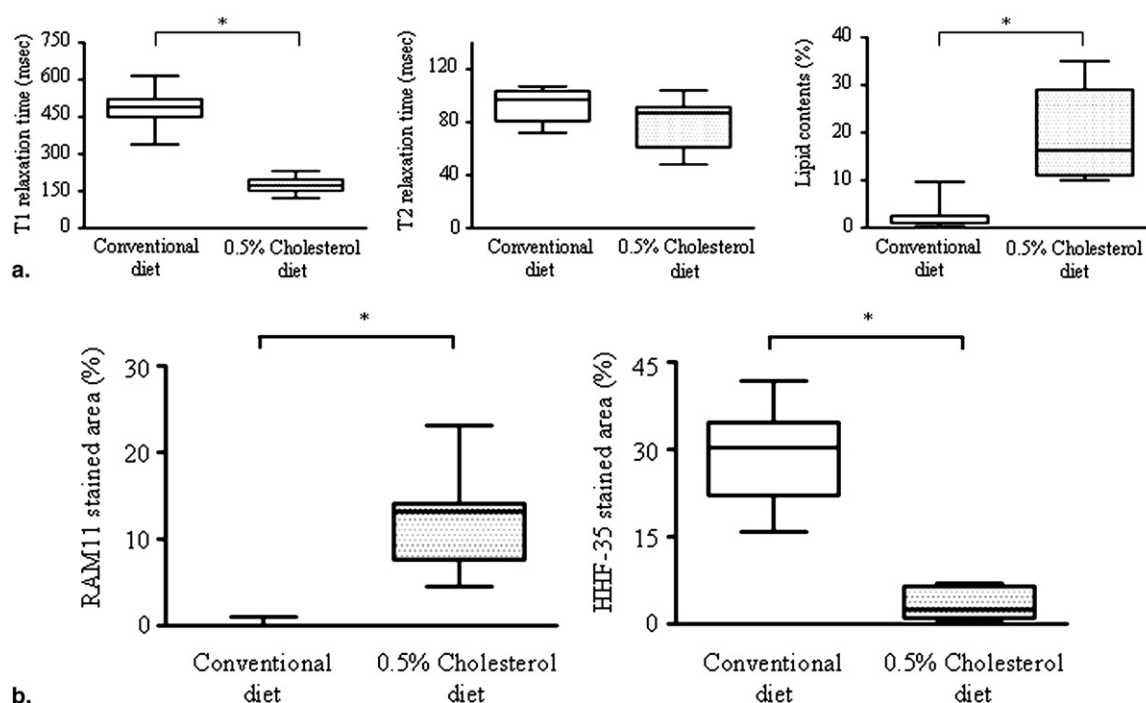


Figure 4. Magnetic resonance parameters ex vivo and linear regression analyses. **(a)** T1 and T2 relaxation times, and lipid contents of iliac arteries in the conventional cholesterol group (CD) (*open box*) and 0.5% cholesterol (ChD) (*dotted box*) groups at 3 weeks after balloon injury ($n = 8$ each; $*P < .001$). **(b)** Immunopositive areas for RAM11 and HHF35 of iliac arteries at 3 weeks after balloon injury in both groups ($n = 8$ each; $*P < .001$). Data are presented as medians (*horizontal bars*), quartile ranges (*boxes*), and 90th percentiles (*error bars*). **(c)** Linear regression analysis of associations between relaxation times and immunopositive area in injured iliac arteries.

Immunostaining controls included non-immune mouse immunoglobulin G instead of the primary antibodies. Areas of positive immunostaining for HHF35 and RAM11 were analyzed using a color imaging morphometry system (Win Roof, Mitani, Fukui, Japan). Briefly, immunopositive areas were extracted using commands to extract colors using specific protocols based on hue, lightness, and saturation. Data are expressed as ratios (%) of immunopositive areas in corresponding areas (13). Two investigators who were blinded to the treatment assignments morphologically analyzed the specimens.

Statistical Analysis

All data are presented as median and range or interquartile range or individual dots. Differences for individual groups were tested using the Mann-Whitney U-test or the Kruskal-Wallis test with Dunn's multiple comparison test (GraphPad Prism 4.03, GraphPad Software Inc, San Diego, CA). The relationships between the factors were evaluated using Spearman's rank correlation coefficient. A P value $< .05$ was considered statistically significant.

RESULTS

Serum Concentrations of TC and TG 4 Weeks after Diets

The serum concentration of TC was significantly higher in rabbits fed with ChD than with CD (median; 697 mg/dL, range;

542–886 mg/dL vs. 46 mg/dL, 21–56 mg/dL, $P < .001$; $n = 3$). The serum TG level was also significantly higher in the rabbits fed with ChD than with CD (median; 272 mg/dL, range; 111–375 mg/dL vs. 13 mg/dL, 3–17 mg/dL, $P < .001$; $n = 3$).

Magnetic Resonance Angiography 3 Weeks after Balloon Injury

Magnetic resonance angiograms of the iliac arteries obtained 3 weeks after balloon injury (left femoral artery) revealed luminal stenosis in both groups of rabbits (Fig 1a-c). Luminal diameters on conventional and magnetic resonance angiographic images of injured arteries significantly and positively correlated (Fig 1d).

MRI in vivo 3 Weeks after Balloon Injury

Figure 2 shows the MRIs, T1 and T2 relaxation times, and lipid content of iliac arteries of the rabbits fed with CD and with ChD. The signal intensity was higher on T1WI, T1 relaxation time was significantly shorter, and lipid content was higher in the injured arteries of the ChD than of the CD group. T2 relaxation time did not significantly differ between the groups.

Histopathological Correlation

Figure 3 shows the histopathological characteristics of the injured iliac arteries of the CD and ChD groups. Neointimal

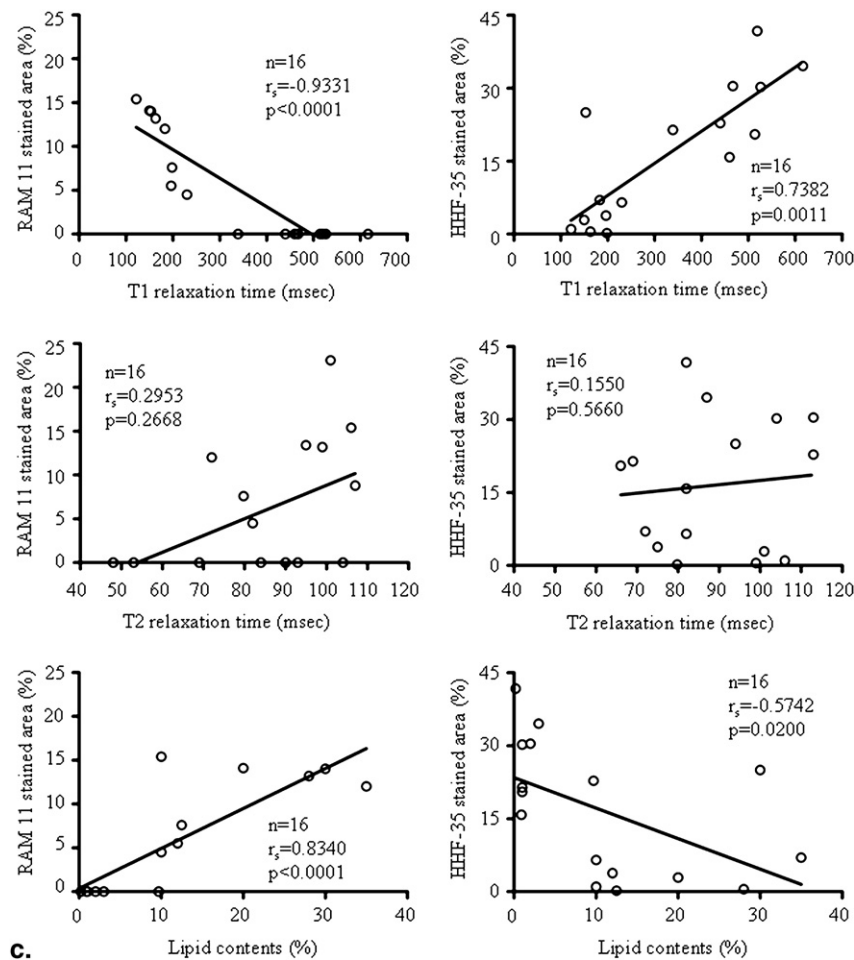


Figure 4. (continued).

formation with luminal stenosis was histologically obvious in the injured arteries of both groups. The neointima of CD group was composed of SMC and extracellular matrix, whereas that of the ChD group comprised macrophages in addition to SMC and extracellular matrix (Fig 3a). The areas immunopositive for RAM11 and for HHF35 in the ChD group were significantly larger and smaller respectively, than those in the CD group (Fig 3b). Replacing primary antibodies with non-immune mouse IgG did not elicit immunoreactivity (data not shown). The T1 relaxation time in the injured arteries negatively or positively correlated with areas immunopositive for RAM11 or for HHF35, respectively. The lipid content in the injured arteries positively or negatively correlated with areas immunopositive for RAM11 or for HHF35, respectively. The T2 relaxation time in the injured arteries did not correlate with the immunopositive areas (Fig 3c).

Ex vivo MRI and Histopathological Correlation

Figure 4 shows the T1 and T2 relaxation times and lipid contents, ex vivo MRIs and histopathological correlations in injured iliac arteries from both groups. The injured arteries of the group fed with ChD showed a significantly shorter T1 relaxation time, more lipid contents and macrophages, and less

SMCs than those of the group fed with CD (Fig 4a, b). The T1 relaxation time in the injured arteries negatively or positively correlated with areas immunopositive for RAM11 or for HHF35, respectively. The lipid content in the injured arteries positively or negatively correlated with areas immunopositive for RAM11 or for HHF35, respectively. The T2 relaxation time in the injured arteries did not correlate with the immunopositive areas (Fig 4c). The results were consistent with those of in vivo study.

DISCUSSION

The present results showed that MRI in vivo can reliably and noninvasively distinguish macrophage- and lipid-rich atherosclerotic, from SMC-rich rabbit arteries, and that macrophage contents in the atherosclerotic artery negatively and positively correlate with T1 relaxation time and lipid content in MRI, respectively.

The risk of thrombotic complication in atherosclerotic arteries depends on plaque composition rather than luminal stenosis (14). The likelihood that unstable plaques will cause thrombotic complications such as myocardial infarction and stroke is high. The histological features of unstable plaques

include a high lipid content, intensive macrophage accumulation, a large necrotic core with a thin fibrous cap and few SMCs, whereas abundant SMCs and fibrous connective tissue characterize stable plaques (15). The degree of luminal stenosis in the iliac arteries of both groups of rabbits was similar at 3 weeks after balloon injury in this study. The injured arteries of the ChD group contained large numbers of foamy macrophages and fewer SMCs in the neointima, whereas the neointima of the arteries in the group fed with CD was composed exclusively of SMCs with fibrous connective tissue. Although a large necrotic core did not develop in the lesioned arteries of the ChD group, these findings are compatible with those of human unstable and stable atherosclerotic plaques (14,15). Therefore, this animal model closely simulates human atherosclerotic vessels.

The T1 relaxation time was significantly shorter and the lipid content was higher in the injured arteries of the ChD, than the CD group both in vivo and ex vivo. Cappendijk et al (16) described that semiquantitative analysis of the lipid-rich necrotic core of carotid atherosclerotic plaques using single-sequence T1-weighted turbo field echo MRI is accurate. The composition of lipids in atherosclerotic lesions (cholesterol esters, cholesterol monohydrate, phospholipids, and triglyceride) changes both chemically and physically with the progression of atherosclerosis (17,18). Yuan et al (19) found that triglyceride and hydrated phospholipids have a high contrast-to-noise ratio on T1WI, whereas cholesterol and cholesterol esters have a low contrast-to-noise ratio at body temperature. Therefore, triglyceride and hydrated phospholipids among the lipids of the injured arteries of ChD group might have affected T1 relaxation time, and allowed quantitation of lipid rich plaque by T1-weighted MRI. Although several studies have shown that T2-weighted contrast MRI can help to distinguish between lipid cores, fibrotic caps, and calcifications (20–22), T2 relaxation time did not significantly differ between macrophage-rich and SMC-rich atherosclerotic vessels in the present study. This might be due to absence of a large necrotic core with a fibrous cap and calcification in this model. Nevertheless, our findings support the notion that MRI can characterize the components of atherosclerotic plaque and support evaluation of plaque vulnerability (23).

T1 relaxation time or lipid contents in injured arteries correlated with areas that were immunopositive for macrophages and SMCs. T1 relaxation time was shorter in macrophage-rich than in SMC-rich atherosclerotic vessels. Helft et al (8,24) reported a significant correlation for plaque composition between MRIs and histopathology in an analysis of lipid and fibrous areas in rabbit aortas. Moreover, the fractional plasma volume and transfer constant of contrast material into the extracellular space correlated with macrophages and neovasculature (25). Although the resolution has potential limitations for imaging such a complex histology of atherosclerotic lesions, the present and previous findings support the notion that MRI can

identify the pathophysiologic characteristics of atherosclerotic plaques. Another limitation of this study is that it is not known whether this study may translate into larger animals like humans.

In conclusion, the present findings suggest that T1-relaxation time would be helpful to distinguish macrophage-rich from SMC-rich plaques. Thus, MRI has considerable potential to assess plaque vulnerability.

REFERENCES

- Davies MJ. Stability and instability: two faces of coronary atherosclerosis. *Circulation* 1996; 94:2013–2020.
- Morteza N, Libby L, Falk E, et al. From vulnerable plaque to vulnerable patient. *Circulation* 2003; 108:1664–1672.
- Fayad ZA, Fuster V. Characterization of atherosclerotic plaques by magnetic resonance imaging. *Ann NY Acad Sci* 2000; 902:173.
- Saam T, Hatsukami TS, Takaya N, et al. The vulnerable, or high-risk, atherosclerotic plaque: noninvasive MR imaging for characterization and assessment. *Radiology* 2007; 244:64–77.
- Yuan C, Mitsumori LM, Ferguson MS, et al. In vivo accuracy of multispectral magnetic resonance imaging for identifying lipid-rich necrotic cores and intraplaque hemorrhage in advanced human carotid plaques. *Circulation* 2001; 104:2051–2056.
- Cai JM, Hatsukami TS, Ferguson MS, et al. Classification of human carotid atherosclerotic lesions with in vivo multicontrast magnetic resonance imaging. *Circulation* 2002; 106:1368–1373.
- Saam T, Ferguson MS, Yarnykh VJ, et al. Quantitative evaluation of carotid plaque composition by in vivo MRI. *Arterioscler Thromb Vasc Biol* 2005; 25:234–239.
- Helt G, Worthley SG, Fuster V, et al. Atherosclerotic aortic component quantification by noninvasive magnetic resonance imaging: an in vivo study in rabbits. *J Am Coll Cardiol* 2001; 37:1149–1154.
- Yamashita A, Furukoji E, Marutsuka K, et al. Increased vascular wall thrombogenicity combined with reduced blood flow promotes occlusive thrombus formation in rabbit femoral artery. *Arterioscler Thromb Vasc Biol* 2004; 24:2420–2424.
- Rasband, W.S., ImageJ, US National Institutes of Health, Bethesda, MD. <http://rsb.info.nih.gov/ij/>, 1997–2008.
- Ishimori Y, Kimura H, Uematsu H, et al. Dynamic T1 estimation of brain tumors using double-echo dynamic MR imaging. *J Magn Reson Imaging* 2003; 18:113–120.
- Griffin JF, Yeung D, Antonio GE, et al. Vertebral marrow fat content and diffusion and perfusion indexes in woman with varying bone density: MR evaluation. *Radiology* 2006; 241:831–838.
- Yamashita A, Shoji K, Tsuruda T, et al. Medial and adventitial macrophages are associated with expansive atherosclerotic remodeling in rabbit femoral artery. *Histol Histopathol* 2008; 23:127–136.
- Fayad ZA, Fuster V. Clinical imaging of the high-risk or vulnerable atherosclerotic plaque. *Circ Res* 2001; 89:305–316.
- Fuster V, Moreno PR, Fayad ZA, et al. Atherothrombosis and high-risk plaque. *J Am Coll Cardiol* 2005; 46:937–954.
- Cappendijk VC, Heeneman S, Kessels A, et al. Comparison of single-sequence T1w TFE MRI with multisequence MRI for the quantification of lipid-rich necrotic core in atherosclerotic plaque. *J Magn Reson Imaging* 2008; 27:1347–1355.
- Katz SS, Shipley GG, Small DM. Physical chemistry of the lipids of human atherosclerotic lesions. Demonstration of a lesion intermediate between fatty streaks and advanced plaques. *J Clin Invest* 1976; 58:200–211.
- Small DM, Shipley GG. Physical-chemical basis of lipid deposition in atherosclerosis. *Science* 1974; 185:222–229.
- Yuan C, Petty C, O'Brien KD, et al. In vitro and in situ magnetic resonance imaging signal features of atherosclerotic plaque-associated lipids. *Arterioscler Thromb Vasc Biol* 1997; 17:1496–1503.
- Yuan C, Tsuruda JS, Beach KN, et al. Techniques for high-resolution MR imaging of atherosclerotic plaque. *J Magn Reson Imaging* 1994; 4:43–49.
- Toussaint JF, Southern JF, Fuster V, et al. T2 contrast for NMR characterization of human atherosclerosis. *Arterioscler Thromb Vasc Biol* 1995; 15:1533–1542.

22. Serfaty JM, Chaabane L, Tabib A, et al. Atherosclerotic plaques: classification and characterization with T2-weighted high-spatial-resolution MR imaging-an in vitro study. *Radiology* 2001; 219:403-410.
23. Saam T, Hatsukami TS, Takaya N, et al. The vulnerable, or high-risk, atherosclerotic plaque: noninvasive MR imaging for characterization and assessment. *Radiology* 2007; 244:64-77.
24. Helft G, Worthley SG, Fuster V, et al. Progression and regression of atherosclerotic lesions: monitoring with serial noninvasive magnetic resonance imaging. *Circulation* 2002; 105:993-998.
25. Kerwin WS, O'Brien KD, Ferguson MS, et al. Inflammation in carotid atherosclerotic plaque: a dynamic contrast-enhanced MR imaging study. *Radiology* 2006; 241:459-468.